Appl Nanosci (2017) 7:155–165
DOI 10.1007/s13204-017-0563-1

ORIGINAL ARTICLE

A molecular dynamics investigation into the adsorption behavior inside {001} kaolinite and {1014} calcite nano-scale channels: the case with confined hydrocarbon liquid, acid gases, and water

Babak Fazelabdolabadi[1] · **Aliasghar Alizadeh-Mojarad**[2]

Received: 11 February 2017 / Accepted: 7 April 2017 / Published online: 12 April 2017

Abstract A set of molecular dynamics simulations was conducted, as the first comparative study of the adsorption behavior of liquid hydrocarbon/acid gases/water molecules over $\{10\bar{1}4\}$ calcite surface and {001} octahedral kaolinite surface in nano-confined slit. According to atomic *z*-density profiles, hydrocarbon molecules have higher tendency towards the $\{10\bar{1}4\}$ calcite surface than the {001} octahedral kaolinite surface. In addition, water molecules form stronger adsorption layer over calcite surface than kaolinite. In contrast, acid gas molecules have higher tendency towards kaolinite surface than calcite. This behavior was spotted within nanometer-sized slit pores. The results also point to reduction in self-diffusion coefficient of molecules with strong adsorption over mineral surfaces in nano-confined environment.

Keywords Molecular dynamics · Calcite · Kaolinite · Nano-confinement

Introduction

As a magnificent analytical tool, molecular dynamics (MD) technique has found its applicability in a diverse spectrum of research. An example of this kind is the study the interaction of carbon dioxide and clay minerals, a matter of potential usage for underground carbon sequestration purposes (Chen et al. 2015a, b, c; Javanbakht et al. 2015; Makaremi et al. 2015; Tenney and Cygan 2014). Another example of the kind is the study of interactions between mineral surfaces (representative of reservoir rocks) and mixture of hydrocarbon/water/acid gases (representing typical reservoir fluids), to put petroleum production industry in target (Chun et al. 2015; Fazelabdolabadi and Alizadeh-Mojarad 2016; Underwood et al. 2015; Wu et al. 2012) or analysis of mobilization and recovery of fluids/asphaltene from nano-pores using MD (Oughanem et al. 2015; Youssef et al. 2015; Stukan et al. 2012). More recently, Xie et al. (2016) studied oil contamination removal process at microscales, using the molecular dynamics technique.

Calcite is composed of carbonate mineral and categorized as mineral materials. Calcite differs from kaolinite (which is known as clay mineral). Clay mineral is a jargon amongst pedologists and it should be distinguished from clay materials. Clay materials exist in nature as fine-grained materials which their size is below 4 μm. Phyllosilicates are only fundamental constituents of clay materials. However, clay mineral materials are both synthetic and natural materials which may contain non-phyllosilicates as their principal component. Clay minerals such as kaolinite have a layered structure, including nanometer-thick layers. Modification of the surface of clay minerals can be done by synthesis methods such as adsorption and grafting (Bergaya et al. 2013).

A plethora of experimental and computational works is available on wetting behavior of reservoir fluids over mineral surfaces, such as quartz (Hou et al. 2015; Saraji et al. 2013; Wu et al. 2013; Xuefen et al. 2009), calcite (Benlia et al. 2012; Cebecia and Sönmezb 2004; Guiwu et al. 2009; Khusainova et al. 2015; Sakuma et al. 2014;

Electronic supplementary material The online version of this article (doi:10.1007/s13204-017-0563-1) contains supplementary material, which is available to authorized users.

✉ Babak Fazelabdolabadi
fazelb@ripi.ir

[1] Institute of Enhanced Oil Recovery, Research Institute of Petroleum Industry (RIPI), West Blvd. Azadi Sports Complex, P.O. Box 14665-1998, Tehran, Iran

[2] Department of Chemical Engineering, University of Tehran, Tehran, Iran

Rezaei Gomari et al. 2006), and kaolinite (Lage et al. 2015; Lebedeva and Fogden 2011; Murgich and Rodríguez 1998; Tabrizy et al. 2011a, b), to ease the conception of the phenomena. Nevertheless, those researches pinpoint to the complexity of wetting behavior existent in different types of minerals. For instance, octahedral and tetrahedral surfaces of {001} kaolinite are discovered with hydrophilic and hydrophobic characteristics, respectively (Ni and Choi 2012; Šolc et al. 2011; Tunega et al. 2004). In addition, hydroxylated surfaces of mineral surfaces can reportedly be different in wetting properties (Chai et al. 2009; Liascukiene et al. 2014). The findings also conclude the wettability and dynamical properties, to be affected by confinement size of pores of reservoir rocks (Al-Quraishi and Khairy 2005; Cui et al. 2003; Standnes and Austad 2000; Yuan et al. 2015). A few investigations were also directed towards analysis of adsorption of organic molecules over clay (Hu et al. 2014; Pernyeszi et al. 1998; Wang et al. 2013) (mainly kaolinite), as well as non-clay (Cooke et al. 2010; de Leeuw and Parker 1998; Freeman et al. 2009; Guiwu et al. 2009; Keller et al. 2015; Sakuma et al. 2014) (mainly calcite) surfaces. In this regards, the main focus has been devoted to the {001} kaolinite or {1014} calcite structures, on the premise of holding the primary cleavage planes (Miller et al. 2007; Sekkal and Zaoui 2013; Titiloye et al. 1993; Zielke et al. 2015).

The present article attempts to address the issue through a comparative framework, to include a mixture of hydrocarbon/acid gas/water in both clay and non-clay environments. The authors, however, are unaware of any available experimental adsorption data with exact correspondence to the simulation systems considered (i.e., fluid composition and type of slit wall); therefore, such comparisons are not attainable at the moment.

Methodology

MD simulations were performed using the LAMMPS simulation package (Plimpton 1995). The simulation considered system was composed of two parts, namely, an immobile (solid) part of mineral structure and a mobile (fluid) part (of hydrocarbon/acid gas/water mixture). OPLS-AA (Optimized Potentials for Liquid Simulations-All Atoms) force field, developed by Jorgensen et al. (1996), was used to describe the interactions among atoms in the hydrocarbon phase. In this work, carbon dioxide (CO_2) and hydrogen sulfide (H_2S) were regarded as acid gas phase. Nath-Escobedo-de Pablo (NERD) (Nath 2003) revised force field and EPM2 potential model (Harris and Yung 1995) was utilized to model H_2S and CO_2, respectively. Extended simple point charge (SPC/E) model of Berendsen et al. (1987) was also used to simulate water molecules. According to SPC/E model, the SHAKE algorithm (Ryckaert et al. 1977) was used to preserve bond and angle geometry constraints for water molecules in the course of MD simulations.

Calcite and kaolinite surfaces were considered as representative of clay and non-clay materials, to form nanoslit walls. In case of calcite surface, $\{10\bar{1}4\}$ calcite structure was utilized, as for being the most stable and neutral surface, to build the 4-nm confined geometry. Neutral octahedral {001} surface of kaolinite was used, as well. To model calcite surfaces, rigid ion model of a force field presented by Pavese et al. (1992, 1996) was employed. The CLAYFF force field (Cygan et al. 2004) was adopted to define all bonded and non-bonded interaction parameters of kaolinite surface. A bread usage of the Pavese and CLAYFF forcefields can be found in recent literature adoptions (Fazelabdolabadi and Alizadeh-Mojarad 2016; Ghatee et al. 2015; Greathouse et al. 2015; Keller et al. 2015; Zielke et al. 2015).

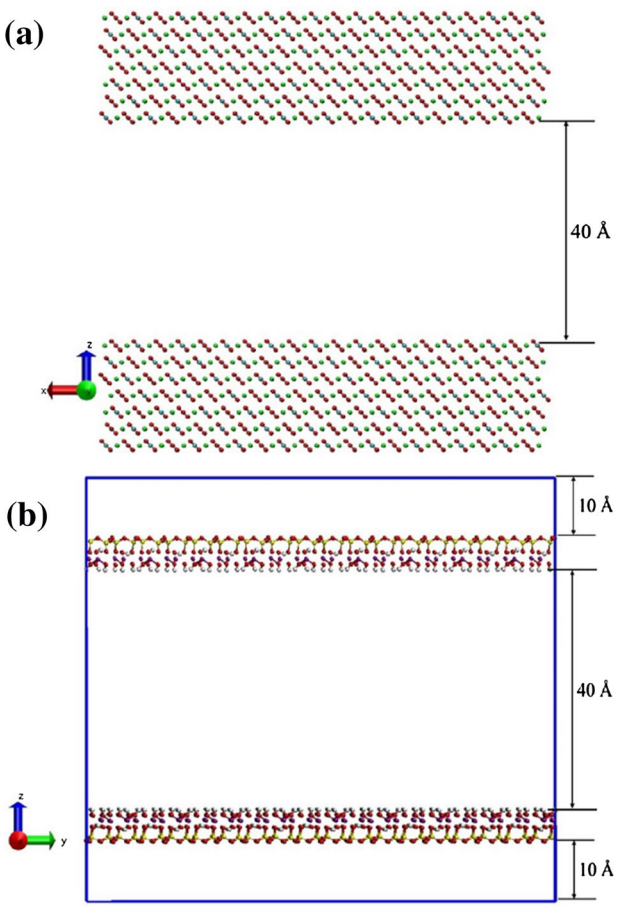

Fig. 1 Rectangular pore configurations for **a** 40 Å calcite pore and **b** 40 Å kaolinite pore. The calcium/carbon/oxygen/hydrogen/aluminum/silicon atoms are shown by *green/blue/red/white/purple/yellow spheres*, respectively

Table 1 Naming convention for the MD simulations

MD simulation	Description
BP-*X*	MD simulation of pure molecules of type *X*[a] under bulk (unconfined) conditions
S1-calcite	MD simulation of confined pure molecules between parallel calcite walls
S1-calcite-*X*	MD simulation results pertaining to molecules of type *X* established under S1-calcite conditions
S1-kaolinite	MD simulation of confined pure molecules between parallel kaolinite walls
S1-kaolinite-*X*	MD simulation results pertaining to molecules of type *X* established under S1-kaolinite conditions
S2-calcite	MD simulation of confined mixture[b] between parallel calcite walls
S2-calcite-*X*	MD simulation results pertaining to molecules of type *X* established under S2-calcite conditions
S2-kaolinite	MD simulation of confined mixture[b] between parallel kaolinite walls
S2-kaolinite-*X*	MD simulation results pertaining to molecules of type *X* established under S2-kaolinite conditions

[a] $X = C_3$ for propane, $X = C_6$ for *n*-hexane, $X = C_7$ for *n*-heptane, $X = C_{10}$ for *n*-decane, $X = CO_2$ for carbon dioxide, $X = H_2O$ for water, and $X = H_2S$ for hydrogen sulfide

[b] Mixture constituents are listed in Table 2

Table 2 Density of molecules for different MD simulations

MD simulation	Molecules' density[a] (#/Å^3)/10^{-3} of S1-calcite-*X*	Molecules' density[a] (#/Å^3)/10^{-3} of S1-kaolinite-*X*
$X = C_3$	0.94	0.94
$X = C_6$	1.60	1.60
$X = C_7$	1.63	1.63
$X = C_{10}$	2.22	2.22
$X = H_2O$	10.20	10.20
$X = H_2S$	4.08	4.08
$X = CO_2$	2.83	2.83

[a] Molecules' density in the *non-crystal* volume of the simulation box

In case of $\{10\bar{1}4\}$ calcite, the methodology suggested by Headen and Boek (2011) was used to describe the van der Waals interaction parameters (to model fluid–solid interface). The van der Waals non-bonded interaction parameters between fluid–solid species in systems, including {001} kaolinite surface, were estimated using the Lorentz–Berthelot mixing rule.

MD simulations were performed under canonical (NVT) ensemble using the Nosé–Hoover thermostat (Hoover 1985; Nosé 1984) with 1 ps relaxation time. Integration of the equations of motion was done every 1 fs. Ewald summation technique was used to calculate electrostatic interactions. The long-range/short-range potentials were truncated at 11 Å distance. Orthorhombic simulation cells were considered with Periodic Boundary Condition (PBC) in *x*–*y* directions. The Packmol package (Martínez et al. 2009) was used to construct the initial configuration of molecules in the simulation cell.

The nano-slit simulation cell constructed was composed of two parallel surfaces, with a 4-nm separation distance (Fig. 1). Two types of surfaces were considered in those regards: the $\{10\bar{1}4\}$ calcite and the {001} kaolinite. The $\{10\bar{1}4\}$ calcite surface contained seven atomic layers (perpendicular to the *z*-direction) in a dimension of 82 Å × 45 Å × 19.30 Å. The {001} octahedral kaolinite surface was composed of 6120 atoms in a dimension of 51.42 Å × 80.40 Å × 5 Å, with its *x*–*y* plane being perpendicular to *z*-direction. For the case of kaolinite walls, two gaps of 10 Å were introduced to the top/bottom ends of the simulation cell, to avoid any unphysical interactions amongst species in the mineral surfaces (Fig. 1b).

Two main systems, namely, S1 and S2, were considered as for the MD simulations. In S1 case, pure molecules are confined between mineral surfaces. In S2 case, mixtures of molecules are placed inside the nano-slit geometry. In addition, molecular dynamics simulations of pure hydrocarbons were performed at bulk conditions over a temperature of 340 K, for further comparison. All MD simulations were attempted under the canonical ensemble.

The time span of MD simulations has been 1 ns (S1 system)/1.5 ns (S2 system). The radius of gyration, R_g, and end-to-end distance were calculated for hydrocarbon

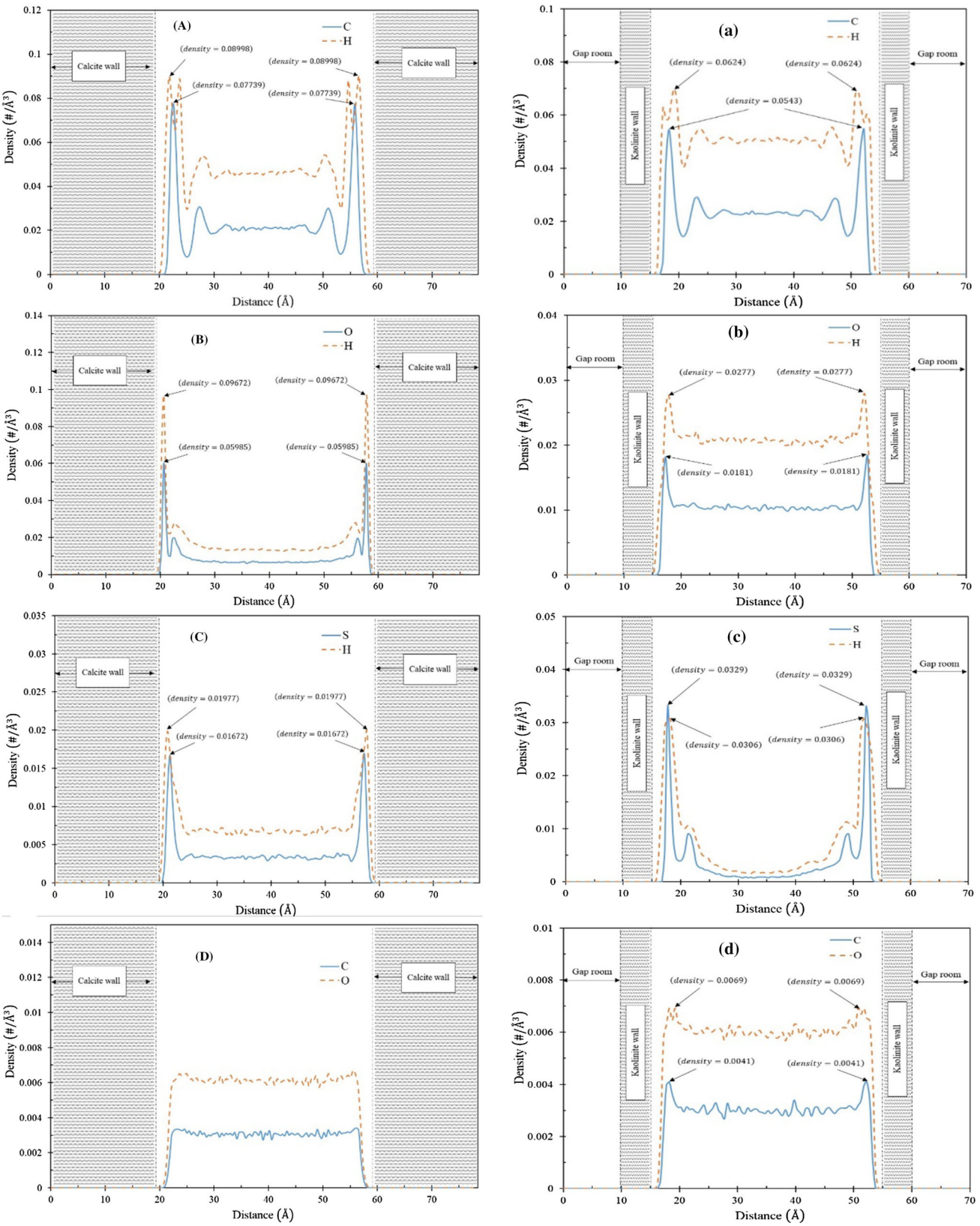

Fig. 2 Atomic *z*-density profiles for **A** S1-calcite-C_{10}, **B** S1-calcite-H_2O, **C** S1-calcite-H_2S, and **D** S1-calcite-CO_2, **a** S1-kaolinite-C_{10}, **b** S1-kaolinite-H_2O, **c** S1-kaolinite-H_2S, and **d** S1-kaolinite-CO_2 simulations at 340 K

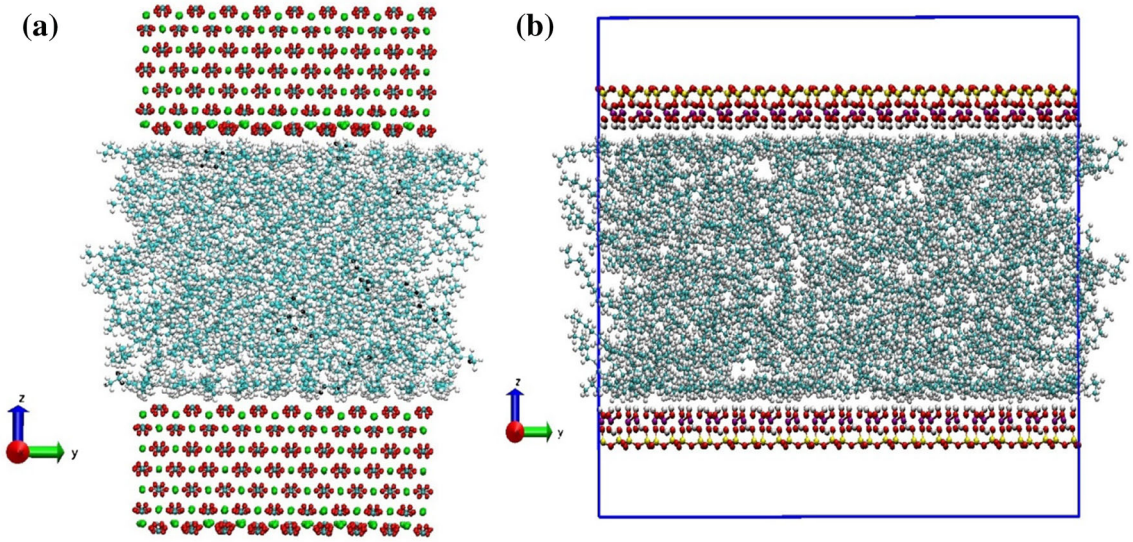

Fig. 3 Final snapshots of molecular distributions for **a** S1-calcite-C_{10} and **b** S1-kaolinite-C_{10}. The calcium/carbon/oxygen/hydrogen/aluminum/silicon atoms are shown by *green/blue/red/white/purple/yellow spheres*, respectively

chains to explain the confinement effect on them. For a given molecule, the radius of gyration was calculated by Eqs. (1) and (2):

$$\vec{r}_{\mathrm{cm}} = \frac{\sum_{i=1}^{n_{\mathrm{segments}}} \vec{r}_i}{n_{\mathrm{segments}}} \tag{1}$$

$$R_{\mathrm{g}} = \left[\frac{\sum_{i=1}^{n_{\mathrm{segments}}} m_i \| \vec{r}_i - \vec{r}_{\mathrm{cm}} \|^2}{\sum_{ii=1}^{n_{\mathrm{segments}}} m_i} \right]^{1/2} \tag{2}$$

where $\vec{r}_{\mathrm{cm}}$ and n_{segments} indicate the (vector) of center-of-mass of a given molecule and the number of (atomic) segments in a molecular chain, respectively. $\vec{r}_i$ and m_i denote, respectively, the (vector) of coordinates and the mass of the iith segment of a given molecule, and $\| \ \|$ represents the vector norm. The mean-squared displacement (MSD) was computed, and the self-diffusion coefficient, D, in different systems studied. Calculation of the self-diffusion coefficient (for a given molecule type) was performed using the Einstein relation (Frenkel and Smit 2011) [Eqs. (3), (4)]:

$$D = \frac{1}{2d} \lim_{t \to \infty} \frac{\mathrm{d} \langle \| \Delta \vec{r}_{\mathrm{cm}}(t) \|^2 \rangle}{\mathrm{d}t} \tag{3}$$

$$\Delta \vec{r}_{\mathrm{cm}}(t) = \frac{\sum_{k=1}^{N} [\vec{r}_{\mathrm{cm}_k}(t) - \vec{r}_{\mathrm{cm}_k}(t=0)]}{N}. \tag{4}$$

Here, $\vec{r}_{\mathrm{cm}_k}$ refers to the vector of center-of-mass of the kth molecule of a given species, for which a total of N molecules exists. In addition, d denotes the dimensionality of the system ($d = 3$), and $\langle \rangle$ indicates the ensemble average of the quantity.

Results and discussion

The naming convention for the (slit) simulations is introduced in Table 1. The information on the composition of molecules considered in mixture states (S2 systems) is also listed in Table 2.

z-Density profiles

Atomic z-density profiles of the MD simulations of S1/S2 systems are presented in Figs. 1 and 2. The position of the calcite and kaolinite walls in each profile has been embedded in the figures, to visually aid the comparison on relative positioning of z-density profiles over the mineral surfaces. S1 system simulations were attempted for propane, hexane, heptanes, and decane molecules. However, for the sake of brevity, only the z-density results for decane are reported herein. The other z-density results can be found in Figs. S-1 and S-2 in the Supplementary Information to this article.

According to z-density profiles of decane and water in calcite nano-slit, two major peaks are appeared. The final configuration of molecules in S1-calcite-C_{10} and S1-kaolinite-C_{10} simulation systems is depicted in Fig. 3. Given the type of molecule under confinement being the same (decane), the adsorption layer over the calcite surface is more ordered state (Fig. 3a) than the kaolinite case (Fig. 3b). The results for confined CO_2 in nano-slit calcite (Fig. 2d) are in perfect agreement with the previous results (Fazelabdolabadi and Alizadeh-Mojarad 2016). The adsorption results for CO_2 (Fig. 2d, D) indicate carbon

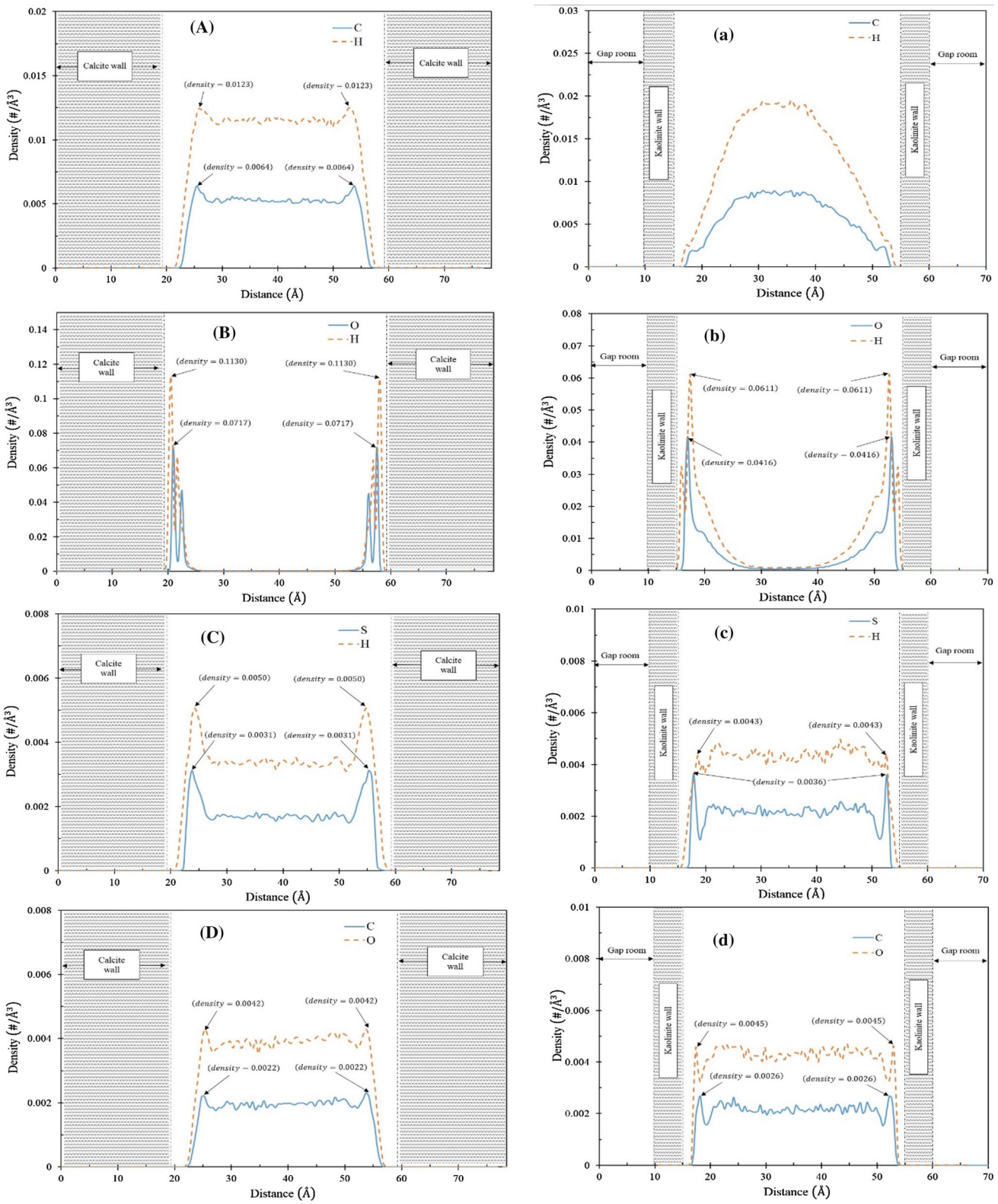

Fig. 4 Atomic z-density profiles for **A** S2-calcite-C_{10}, **B** S2-calcite-H_2O, **C** S2-calcite-H_2S, and **D** S2-calcite-CO_2, **a** S2-kaolinite-C_{10}, **b** S2-kaolinite-H_2O, **c** S2-kaolinite-H_2S, and **d** S2-kaolinite-CO_2 simulations at 340 K

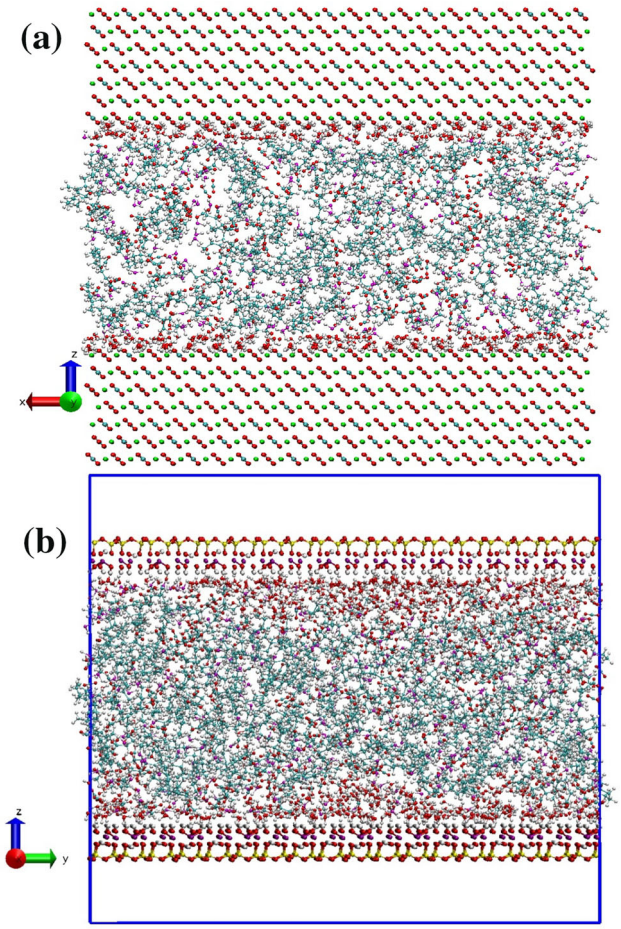

Fig. 5 Final snapshots of molecular distributions for **a** S2-calcite and **b** S2-kaolinite. The calcium/carbon/oxygen/hydrogen/sulfur/aluminum/silicon atoms are shown by *green/blue/red/white/magenta/purple/yellow spheres*, respectively

dioxide to have stronger tendency towards hydrophilic {001} octahedral kaolinite surface than $\{10\bar{1}4\}$ calcite surface, with the same value of CO_2 density. A similar trend is for H_2S, with the density of hydrogen sulfide being kept equal in both the systems (Fig. 2C, c). The trend is somehow reversed for the water case; and H_2O has more tendency for adsorption onto the calcite surface than {001} octahedral kaolinite (Fig. 2B, b). The results for z-density of oxygen atoms over {001} octahedral kaolinite surface are in good agreement with previous computational reports (Feibelman 2013; Tunega et al. 2004).

The adsorption profiles (Fig. 4), obtained by MD simulations, were calculated for the S2 systems (with mixture of molecules being under slit confinement). For the sake of comparison, the density of molecules is kept the same, between the systems of different wall types. Visual inspection of the final configuration of molecules in systems (Fig. 5) may lead us to an important finding that adsorption layer of water molecules over calcite surface (in S2 systems) looks more ordered than its adsorption layer counterpart over the kaolinite surface, albeit kaolinite's hydrophilicity. The accumulation of hydrocarbon molecules in the middle of simulation box can be a result of hydrophilicity of {001} octahedral kaolinite surface and this behavior is in agreement with previous results (Ni and Choi 2012). To obtain accurate results, the system should have reached equilibrium prior to sampling the simulation box. For the sake, we followed the standard protocol, and monitored the system's temperature and energy versus simulation time, to ensure equilibrium. The data are presented in the Supplementary Information to this article.

Table 3 Average radius of gyration, $\langle R_g \rangle$ (Å), for different MD simulations

	BP-*X*	S1-calcite-*X*	S1-kaolinite-*X*	S2-calcite-*X*	S2-kaolinite-*X*
$X = C_3$	1.25 ± 0.07	1.24 ± 0.04	1.25 ± 0.04	1.24 ± 0.03	1.25 ± 0.02
$X = C_6$	1.92 ± 0.05	1.87 ± 0.03	1.89 ± 0.13	1.89 ± 0.13	1.90 ± 0.09
$X = C_7$	2.59 ± 0.06	2.50 ± 0.13	2.53 ± 0.06	2.50 ± 0.11	2.53 ± 0.12
$X = C_{10}$	3.59 ± 0.09	3.43 ± 0.21	3.49 ± 0.08	3.35 ± 0.23	3.40 ± 0.20

Table 4 Average end-to-end distance (Å) for different MD simulations

	BP-*X*	S1-calcite-*X*	S1-kaolinite-*X*	S2-calcite-*X*	S2-kaolinite-*X*
$X = C_3$	2.44 ± 0.08	2.43 ± 0.10	2.44 ± 0.11	2.43 ± 0.08	2.43 ± 0.05
$X = C_6$	6.04 ± 0.05	5.09 ± 0.22	6.02 ± 0.57	5.86 ± 0.55	5.96 ± 0.46
$X = C_7$	7.25 ± 0.03	6.93 ± 0.85	6.98 ± 0.68	6.90 ± 0.69	6.95 ± 0.84
$X = C_{10}$	10.45 ± 0.30	10.23 ± 1.43	10.44 ± 1.34	9.98 ± 1.49	10.32 ± 1.08

Table 5 Self-diffusion coefficient $D_{H2O}(10^{-9}\ m^2s^{-1})$ for different MD simulations at 340 K

	S1-calcite-*X*	S1-kaolinite-*X*	S2-calcite-*X*	S2-kaolinite-*X*
$X = C_3$	373.88	517.93	34.64	12.34
$X = C_6$	52.96	71.24	22.49	11.17
$X = C_7$	42.90	48.57	16.58	12.10
$X = C_{10}$	9.29	9.69	9.18	9.05
$X = H_2O$	141.80	145.46	7.63	12.98
$X = H_2S$	260.83	49.31	44.54	20.95
$X = CO_2$	455.89	399.715	46.40	21.96

In case of acid gases, the change in type of the slit wall (S2 systems) seems to alter the arrangement of H atoms in vicinity of the surfaces by comparing the *z*-density profiles of hydrogen atoms in Fig. 4C, c and D, d. The simulation findings on the tendency of hydrocarbon, acid gases, and water towards the calcite surface are also in agreement with published experimental reports (Broseta et al. 2012; Karoussi and Hamouda 2008; Tabrizy et al. 2011a, b).

Radius of gyration and end-to-end distance

The radius of gyration ($\langle R_g \rangle$) and end-to-end distance of molecules were computed under canonical ensemble, and are reported in Tables 3 and 4. The results are in good agreement to previous reports on pure hydrocarbons (modeled using United-Atom or All-Atom force fields) (Feng et al. 2013; Ferguson et al. 2009; Thomas et al. 2006). Comparison against the bulk-configuration results shows reduction in these properties, which is more conspicuous for longer chain hydrocarbons. This change in conformation of molecules should be regarded as an apparent effect of nano-slit confinement.

Self-diffusion

Calculation of the ensemble average of the mean square displacement (MSD) of center-of-mass of each molecule type was attempted every 4 ps. The data were subsequently used to establish the two-dimensional self-diffusion coefficient of molecules, using Eqs. (3) and (4). Table 5 lists the computed self-diffusion values under each wall type. A huge reduction in diffusion coefficient is seen, for example, for H_2O, in shifting to mixture state (S2 system). This can be described by strong adsorption of water molecules over S2-calcite/S2-kaolinite than S1-calcite/S1-kaolinite. However, in comparison, less water molecules are adsorbed over the kaolinite surface, giving the molecules more freedom of movement, and hence, a larger value for diffusion coefficient is obtained for kaolinite case with water. The phenomenon is somehow reversed for acid gases in mixture state, with less acid gases being adsorbed onto calcite surface, resulting to a more freedom of movement and increased value in self-diffusion of acid gases in S2-calcite systems. A similar argument may be put forward, to describe the change-in-value for hydrocarbons.

Conclusions

MD simulation results of pure molecules (S1-calcite/S1-kaolinite systems) indicate water to have higher tendency to be adsorbed over the {1014} calcite surface than {001} octahedral kaolinite surface and supported by two distinct layers of adsorption. Acid gases follow the opposite trend of having more tendency of being adsorbed over the kaolinite surface than calcite. The existence of a middle-region water phase was also ruled out in a 40-Å calcite slit-pore in (S2 systems). The change in the radius of gyration and end-to-end distance of hydrocarbon molecules should be attributed to a conformational change induced by confinement in nano-slit environment. The change-in-value of diffusion coefficients can be attributed to different levels of molecular adsorptions, with higher freedom of movement from less adsorption onto system walls, which results in a higher value diffusion coefficient.

References

Al-Quraishi A, Khairy M (2005) Pore pressure versus confining pressure and their effect on oil–water relative permeability curves. J Petrol Sci Eng 48(1–2):120–126. doi:10.1016/j.petrol.2005.04.006

Benlia B, Dub H, Sabri Celika M (2012) The anisotropic characteristics of natural fibrous sepiolite as revealed by contact angle,

surface free energy, AFM and molecular dynamics simulation. Colloids Surf A 408:22–31. doi:10.1016/j.colsurfa.2012.04.018
Berendsen HJC, Grigera JR, Straatsma TP (1987) The missing term in effective pair potentials. J Phys Chem 91(24):6269–6271. doi:10.1021/j100308a038
Bergaya F, Theng BKG, Lagaly G (eds) (2013) Handbook of clay science. Developments of clay science, vol 1. Elsevier, Amsterdam
Broseta D, Tonnet N, Shah V (2012) Are rocks still water-wet in the presence of dense CO_2 or H_2S? Geofluids 12(4):280–294. doi:10.1111/j.1468-8123.2012.00369.x
Cebecia Y, Sönmezb I (2004) A study on the relationship between critical surface tension of wetting and oil agglomeration recovery of calcite. J Colloid Interf Sci 273(1):300–305. doi:10.1016/j.jcis.2004.01.032
Chai J, Liu S, Yang X (2009) Molecular dynamics simulation of wetting on modified amorphous silica surface. Appl Surf Sci 255(22):9078–9084. doi:10.1016/j.apsusc.2009.06.109
Chen C, Wan J, Li W, Song Y (2015a) Water contact angles on quartz surfaces under supercritical CO2 sequestration conditions: experimental and molecular dynamics simulation studies. Int J Greenh Gas Control 42:655–665. doi:10.1016/j.ijggc.2015.09.019
Chen C, Zhang N, Li W, Song Y (2015b) Water contact angle dependence with hydroxyl functional groups on silica surfaces under CO_2 sequestration conditions. Environ Sci Technol 49(24):14680–14687. doi:10.1021/acs.est.5b03646
Chen J, Si H, Chen W (2015c) Molecular dynamics study of oil detachment from an amorphous silica surface in water medium. Appl Surf Sci 353:670–678. doi:10.1016/j.apsusc.2015.06.138
Chun BJ, Lee SG, Choi JI, Jang SS (2015) Adsorption of carboxylate on calcium carbonate $(10\bar{1}4)$ surface: molecular simulation approach. Colloid Surf A 474:9–17. doi:10.1016/j.colsurfa.2015.03.003
Cooke DJ, Gray RJ, Sand KK, Stipp SL, Elliott JA (2010) Interaction of ethanol and water with the 1014 surface of calcite. Langmuir 26(18):14520–14529. doi:10.1021/la100670k
Cui ST, McCabe C, Cummings PT, Cochran HD (2003) Molecular dynamics study of the nano-rheology of *n*-dodecane confined between planar surfaces. J Chem Phys 118:8941. doi:10.1063/1.1568084
Cygan RT, Liang J, Kalinichev AG (2004) Molecular models of hydroxide, oxyhydroxide, and clay phases and the development of a general force field. J Phys Chem B 108(4):1255–1266. doi:10.1021/jp0363287
de Leeuw NH, Parker SC (1998) Modeling the competitive adsorption of water and methanoic acid on calcite and fluorite surfaces. Langmuir 14(20):5900–5906. doi:10.1021/la980269k
Fazelabdolabadi B, Alizadeh-Mojarad A (2016) On the adsorption and hydrodynamics behavior of H_2S and CO_2 molecules in organic liquids inside nanoslit pores in vicinity of calcite 1014 surface. J Nat Gas Sci Eng 28:106–120. doi:10.1016/j.jngse.2015.11.023
Feibelman PJ (2013) Viscosity of ultrathin water films confined between aluminol surfaces of kaolinite: ab initio simulations. J Phys Chem C 117(12):6088–6095. doi:10.1021/jp312152h
Feng H, Gao W, Sun Z, Lei B, Li G, Chen L (2013) Molecular dynamics simulation of diffusion and structure of some *n*-alkanes in near critical and supercritical carbon dioxide at infinite dilution. J Phys Chem B 117(41):12525–12534. doi:10.1021/jp401824d
Ferguson AL, Debenedetti PG, Panagiotopoulos AZ (2009) Solubility and molecular conformations of *n*-alkane chains in water. J Phys Chem B 113(18):6405–6414. doi:10.1021/jp811229q
Freeman CL, Asteriadis L, Yang M, Harding JH (2009) Interactions of organic molecules with calcite and magnesite surfaces. J Phys Chem C 113(9):3666–3673. doi:10.1021/jp807051u
Frenkel D, Smit B (2011) Understanding molecular simulation: from algorithms to applications. Academic Press, San Diego
Ghatee MH, Koleini MM, Ayatollahi S (2015) Molecular dynamics simulation investigation of hexanoic acid adsorption onto calcite (1014) surface. Fluid Phase Equilib 387:24–31. doi:10.1016/j.fluid.2014.11.029
Greathouse JA, Geatches DL, Pike DQ Christopher, Greenwell HC, Johnston CT, Wilcox J, Cygan RT (2015) Methylene blue adsorption on the basal surfaces of kaolinite: structure and thermodynamics from quantum and classical molecular simulation. Clay Clay Miner 63(3):185–198. doi:10.1346/CCMN.2015.0630303
Guiwu L, Zhang X, Shao C, Yang H (2009) Molecular dynamics simulation of adsorption of an oil–water–surfactant mixture on calcite surface. Pet Sci 6(1):76–81. doi:10.1007/s12182-009-0014-z
Harris JG, Yung KH (1995) Carbon dioxide's liquid-vapor coexistence curve and critical properties as predicted by a simple molecular model. J Phys Chem 99(31):12021–12024. doi:10.1021/j100031a034
Headen TF, Boek ES (2011) Molecular dynamics simulations of asphaltene aggregation in supercritical carbon dioxide with and without limonene. Energy Fuels 25(2):503–508. doi:10.1021/ef1010397
Hoover WG (1985) Canonical dynamics: equilibrium phase-space distributions. Phys Rev A 31:1695. doi:10.1103/PhysRevA.31.1695
Hou B, Wang Y, Huang Y (2015) Mechanistic study of wettability alteration of oil-wet sandstone surface using different surfactants. Appl Surf Sci 330:56–64. doi:10.1016/j.apsusc.2014.12.185
Hu M, Cheng Z, Zhang M, Liu M, Song L, Zhang Y, Li J (2014) Effect of calcite, kaolinite, gypsum, and montmorillonite on Huadian oil shale kerogen pyrolysis. Energy Fuels 28(3):1860–1867. doi:10.1021/ef4024417
Javanbakht G, Sedghi M, Welch W, Goual L (2015) Molecular dynamics simulations of CO_2/water/quartz interfacial properties: impact of CO_2 dissolution in water. Langmuir 31(21):5812–5819. doi:10.1021/acs.langmuir.5b00445
Jorgensen WL, Maxwell DS, Tirado-Rives J (1996) Development and testing of the OPLS all-atom force field on conformational energetics and properties of organic liquids. J Am Chem Soc 118(45):11225–11236. doi:10.1021/ja9621760
Karoussi O, Hamouda AA (2008) Macroscopic and nanoscale study of wettability alteration of oil-wet calcite surface in presence of magnesium and sulfate ions. J Colloid Interf Sci 317(1):26–34. doi:10.1016/j.jcis.2007.09.045
Keller KS, Olsson MHM, Yang M, Stipp SLS (2015) Adsorption of ethanol and water on calcite: dependence on surface geometry and effect on surface behavior. Langmuir 31(13):3847–3853. doi:10.1021/la504319z
Khusainova A, Nielsen SM, Pedersen HH, Woodley JM, Shapiro A (2015) Study of wettability of calcite surfaces using oil–brine–enzyme systems for enhanced oil recovery applications. J Petrol Sci Eng 127:53–64. doi:10.1016/j.petrol.2014.12.014
Lage MR, Stoyanov SR, de Mesquita Walkimar, Carneiro J, Dabros T, Kovalenko A (2015) Adsorption of bitumen model compounds on kaolinite in liquid and supercritical carbon dioxide solvents: a study by periodic density functional theory and molecular theory of solvation. Energy Fuels 29(5):2853–2863. doi:10.1021/ef502202q

Lebedeva EV, Fogden A (2011) Wettability alteration of kaolinite exposed to crude oil in salt solutions. Colloid Surf A 377(1–3):115–122. doi:10.1016/j.colsurfa.2010.12.051

Liascukiene I, Steffenhagen M, Asadauskas SJ, Lambert J, Landoulsi J (2014) Self-assembly of fatty acids on hydroxylated Al surface and effects of their stability on wettability and nanoscale organization. Langmuir 30(20):5797–5807. doi:10.1021/la404756y

Makaremi M, Jordan KD, Guthrie GD, Myshakin EM (2015) Multiphase Monte Carlo and molecular dynamics simulations of water and CO_2 intercalation in montmorillonite and beidellite. J Phys Chem C 119(27):15112–15124. doi:10.1021/acs.jpcc.5b01754

Martínez L, Andrade R, Birgin EG, Martínez JM (2009) PACKMOL: a package for building initial configurations for molecular dynamics simulations. J Comput Chem 30(13):2157–2164. doi:10.1002/jcc.21224

Miller JD, Nalaskowski J, Abdul B, Du H (2007) Surface characteristics of kaolinite and other selected two layer silicate minerals. Can J Chem Eng 85(5):617–624. doi:10.1002/cjce.5450850508

Murgich J, Rodríguez MJ (1998) Interatomic interactions in the adsorption of asphaltenes and resins on kaolinite calculated by molecular dynamics. Energy Fuels 12(2):339–343. doi:10.1021/ef9701302

Nath SK (2003) Molecular simulation of vapor–liquid phase equilibria of hydrogen sulfide and its mixtures with alkanes. J Phys Chem B 107(35):9498–9504. doi:10.1021/jp034140h

Ni X, Choi P (2012) Wetting behavior of nanoscale thin films of selected organic compounds and water on model basal surfaces of kaolinite. J Phys Chem C 116(50):26275–26283. doi:10.1021/jp305223w

Nosé S (1984) A unified formulation of the constant temperature molecular dynamics methods. J Chem Phys 81:511. doi:10.1063/1.447334

Oughanem R, Youssef S, Bauer D, Peysson Y, Maire E, Vizika O (2015) A multi-scale investigation of pore structure impact on the mobilization of trapped oil by surfactant injection. Transp Porous Med 109(3):673–692. doi:10.1007/s11242-015-0542-5

Pavese A, Catti M, Price GD, Jackson RA (1992) Interatomic potentials for $CaCO_3$ polymorphs (calcite and aragonite), fitted to elastic and vibrational data. Phys Chem Miner 19(2):80–87. doi:10.1007/BF00198605

Pavese A, Catti M, Parker SC, Wall A (1996) Modelling of the thermal dependence of structural and elastic properties of calcite, $CaCO_3$. Phys Chem Miner 23(2):89–93. doi:10.1007/BF00202303

Pernyeszi T, Patzko A, Berkesi O, Dékány I (1998) Asphaltene adsorption on clays and crude oil reservoir rocks. Colloid Surf A 137(1):373–384. doi:10.1016/S0927-7757(98)00214-3

Plimpton S (1995) Fast parallel algorithms for short-range molecular dynamics. J Comput Phys 117(1):1–19. doi:10.1006/jcph.1995.1039

Rezaei Gomari KA, Denoyel R, Hamouda AA (2006) Wettability of calcite and mica modified by different long-chain fatty acids (C18 acids). J Colloid Interf Sci 297(2):470–479. doi:10.1016/j.jcis.2005.11.036

Ryckaert JP, Ciccotti G, Berendsen HJ (1977) Numerical integration of the Cartesian equations of motion of a system with constraints: molecular dynamics of *n*-alkanes. J Comput Phys 23(3):327–341. doi:10.1016/0021-9991(77)90098-5

Sakuma H, Andersson MP, Bechgaard K, Stipp SLS (2014) Surface tension alteration on calcite, induced by ion substitution. J Phys Chem C 118(6):3078–3087. doi:10.1021/jp411151u

Saraji S, Goual L, Piri M, Plancher H (2013) Wettability of supercritical carbon dioxide/water/quartz systems: simultaneous measurement of contact angle and interfacial tension at reservoir conditions. Langmuir 29(23):6856–6866. doi:10.1021/la3050863

Sekkal W, Zaoui A (2013) Nanoscale analysis of the morphology and surface stability of calcium carbonate polymorphs. Sci Rep 3:1587. doi:10.1038/srep01587

Šolc R, Gerzabek MH, Lischka H, Tunega D (2011) Wettability of kaolinite (001) surfaces—molecular dynamic study. Geoderma 169:47–54. doi:10.1016/j.geoderma.2011.02.004

Standnes DC, Austad T (2000) Wettability alteration in chalk: 1. Preparation of core material and oil properties. J Pet Sci Eng 28(3):111–121. doi:10.1016/S0920-4105(00)00083-8

Stukan MR, Ligneul P, Boek ES (2012) Molecular dynamics simulation of spontaneous imbibition in nanopores and recovery of asphaltenic crude oils using surfactants for EOR applications. Oil Gas Sci Technol 67(5):737–742. doi:10.2516/ogst/2012039

Tabrizy VA, Denoyel R, Hamouda AA (2011a) Characterization of wettability alteration of calcite, quartz and kaolinite: surface energy analysis. Colloid Surf A 384(1):98–108. doi:10.1016/j.colsurfa.2011.03.021

Tabrizy VA, Hamouda AA, Denoyel R (2011b) Influence of magnesium and sulfate ions on wettability alteration of calcite, quartz, and kaolinite: surface energy analysis. Energy Fuels 25(4):1667–1680. doi:10.1021/ef200039m

Tenney CM, Cygan RT (2014) Molecular simulation of carbon dioxide, brine, and clay mineral interactions and determination of contact angles. Environ Sci Technol 48(3):2035–2042. doi:10.1021/es404075k

Thomas LL, Christakis TJ, Jorgensen WL (2006) Conformation of alkanes in the gas phase and pure liquids. J Phys Chem B 110(42):21198–21204. doi:10.1021/jp064811m

Titiloye JO, Parker SC, Mann S (1993) Atomistic simulation of calcite surfaces and the influence of growth additives on their morphology. J Cryst Growth 131(3):533–545. doi:10.1016/0022-0248(93)90205-B

Tunega D, Gerzabek MH, Lischka H (2004) Ab initio molecular dynamics study of a monomolecular water layer on octahedral and tetrahedral kaolinite surfaces. J Phys Chem B 108(19):5930–5936. doi:10.1021/jp037121g

Underwood T, Erastova V, Cubillas P, Greenwell HC (2015) Molecular dynamic simulations of montmorillonite-organic interactions under varying salinity: an insight into enhanced oil recovery. J Phys Chem C 119(13):7282–7294. doi:10.1021/acs.jpcc.5b00555

Wang S, Liu Q, Tan X, Xu C, Gray MR (2013) Study of asphaltene adsorption on kaolinite by X-ray photoelectron spectroscopy and time-of-flight secondary ion mass spectroscopy. Energy Fuels 27(5):2465–2473. doi:10.1021/ef4001314

Wu J, He J, Torsater O, Zhang Z (2012) Effect of nanoparticles on oil–water flow in a confined nanochannel: a molecular dynamics study. In: SPE international oilfield nanotechnology conference and exhibition. Society of Petroleum Engineers. doi:10.2118/156995-MS

Wu G, He L, Chen D (2013) Sorption and distribution of asphaltene, resin, aromatic and saturate fractions of heavy crude oil on quartz surface: molecular dynamic simulation. Chemosphere 92(11):1465–1471. doi:10.1016/j.chemosphere.2013.03.057

Xie W, Sun Y, Liu H, Fu H, Liang Y (2016) Conformational change of oil contaminants adhered onto crystalline alpha-alumina surface in aqueous solution. Appl Surf Sci 360(A):184–191. doi:10.1016/j.apsusc.2015.10.168

Xuefen Z, Guiwu L, Xiaoming W, Hong Y (2009) Molecular dynamics investigation into the adsorption of oil–water–surfactant mixture on quartz. Appl Surf Sci 255(13):6493–6498. doi:10.1016/j.apsusc.2009.02.021

Youssef S, Oughanem R, Peysson Y, Bauer D, Vizika O (2015) Mobilization of trapped oil by surfactant injection-an

experimental study using multi-scale imaging. In: IOR 2015-18th European symposium on improved oil recovery. doi:10.3997/2214-4609.201412161

Yuan Q, Zhu X, Lin K, Zhao YP (2015) Molecular dynamics simulations of the enhanced recovery of confined methane with carbon dioxide. Phys Chem Chem Phys 17(47):31887–31893. doi:10.1039/C5CP06649B

Zielke SA, Bertram AK, Patey GN (2015) Simulations of ice nucleation by kaolinite (001) with rigid and flexible surfaces. J Phys Chem B. Article ASAP. doi:10.1021/acs.jpcb.5b09052